ELSEVIER

Microelectronic Engineering 53 (2000) 133–136

MICROELECTRONIC ENGINEERING

www.elsevier.nl/locate/mee

$AlSi_xN_y$ as an Embedded Layer for Attenuated Phase-Shifting Mask in 193 nm and the Utilization of a Chemically Amplified Negative Resist NEB-22 for Maskmaking

Wen-an Loong and Cheng-ming Lin

Institute of Applied Chemistry, National Chiao Tung University, Hsinchu 30010, Taiwan, Republic of China

$AlSi_xN_y$ (x~0.31, y~0.45) thin film as a new embedded material for AttPSM in 193 nm lithography was presented. With the good controlling of plasma sputtering of Al (100~130 W) and Si (20~50 W) under Ar (75 sccm), and nitrogen (2.5~5 sccm), $AlSi_xN_y$ has enough deposition latitude to meet the requirements as an embedded layer. For required phase shift 180 degree, the calculated thickness d_{180} of $AlSi_xN_y$ films is in the range of 87~100 nm. The T% in 365 and 488 nm for optical inspection and alignment is below 40%. Its sheet resistance R_s, is less than 0.8 kΩ/square. Helicon wave plasma etcher and Taguchi design of experiment have been applied to the study of the etching selectivity of $AlSi_xN_y$ over substrate fused silica and negative resist NEB-22. Under chamber pressure 3 mtorr, BCl_3 45 sccm, Cl_2 7 sccm, plasma source power 1400 W and substrate bias RF power 30 W for the selectivity of $AlSi_xN_y$ over NEB-22 was found to be 4.8:1. The selectivity of $AlSi_xN_y$ over fused silica was 12.3:1 under chamber pressure 9 mtorr, BCl_3 13 sccm, Cl_2 45 sccm, O_2 8 sccm, plasma source power 1400 W and substrate bias RF power 30 W. A 0.3 μm line/space etched pattern using $AlSi_xN_y$ as embedded layer was successfully fabricated.

1. Introduction

We have reported a series of Ti-based materials as new embedded materials for AttPSM [1]. In this paper, $AlSi_xN_y$ thin film as a new embedded material suitable for AttPSM in 193 nm was presented. Our modified R-T (reflectance-transmittance) method and commercial n-k analyzer were used for the determination of n and k of this thin film. A helicon wave plasma etcher, operated at low pressure, was used to study the etching selectivity of $AlSi_xN_y$ over substrate fused silica and chemically amplified negative resist NEB-22. Taguchi methodology of design of experiment has been applied to obtain the optimal etching conditions. A 0.3 μm line/space etched pattern on fused silica using $AlSi_xN_y$ thin film as embedded layer was successfully fabricated.

2. Experimental

$AlSi_xN_y$ films were deposited on substrates of fused silica or SiO_2/Si wafer under Al (100~130 W), Si (20~50 W), Ar (75 sccm) and nitrogen (2.5~5 sccm) with an Ion Tech Merovac 450C sputtering system. The deposition rate of these thin films was 7.8~10.6 nm/min. Transmittance T% and reflectance R% were taken from a Shimadsu UV-2501PC double-beam UV-VIS spectrometer. Thickness of embedded layer and silicon oxide was measured using a Dektak 3030 surface profilometer and a n&k Technology NKT 1200 analyzer. The resist thickness was measured with a Nano Spec/AFT Models 210UV thin film measurement system. The Ion depth profiles of these thin films were analyzed by a Cameca IMS-5F secondary ion mass spectrometer (SIMS) using O_2^+ as ion source under 12.5 kV and 20,000 mass resolution power. Sheet resistance R_s was measured using a Napson RT-7 resistance analyzer. Micrographs were taken by a Hitachi S-400 FE-SEM and a Hitachi S-6260H in line CC-FE SEM. Atomic force microscope (AFM) used is a Digital Instruments D5000. The chemical composition of thin film surface was analyzed with a VG Microlab 310F Electron Spectroscopy for Chemical Analysis (ESCA) using Mg K_α standard source under scan 1 eV. The atomic ratios of thin films were analyzed with a Joel JXA-8800M EPMA (Electron Probe X-Ray Microanalyzer). The cleaning durability of these thin films was studied by the following three steps. These films were etched by plasma with 80 W O_2 for

0167-9317/00/$ – see front matter
PII: S0167-9317(00)00280-X

5 min; then soaked in SVC-150 resist stripper at 80°C for 30 min; and finally, rinsed in DI water with a BRANSONIC 1200 ultrasonic cleaner at 80°C for 30 min.

The lithographic pattern of $AlSi_xN_y$ embedded layer was carried out by a Leica EBML-300 e-beam exposure system. An Anelva ILD-4100 helicon wave etcher using O_2+BCl_3/Cl_2 as etchants was used to study the etching selectivity and fabricate the etched pattern of $AlSi_xN_y$ embedded layer.

3. Results and Discussion

3.1 Optical and Physical Properties

The n, k plane of $AlSi_xN_y$ thin film was shown in Fig. 1 which including the window suitable as embedded material in 193 nm. For required phase shift 180 degree, the calculated thickness d_{180} of $AlSi_xN_y$ films is in the range of 87~100 nm. The T% in 365 and 488 nm for optical inspection and alignment is smaller than 40%. The measured R_s is less than 0.8 kΩ/square at thickness of d_{180}, suitable for e-beam direct-write.

In order to achieve the required optical window for an embedded material, n and k of $AlSi_xN_y$ films should be well controlled. By changing the N_2 flow rate percentage from 3.2% to 6.3% in the N_2 and Ar mixed gases, as shown in Fig. 1, $AlSi_xN_y$ films can meet the required window. With the increasing of N_2 flow rate, the n of $AlSi_xN_y$ films increases and the k decreases. Compared to Al/AlN bi-layer embedded material [2], $AlSi_xN_y$ films have much larger film deposition latitude to meet the optical requirements for AttPSM.

The increasing of atomic percentage of nitrogen in $AlSi_xN_y$ films was in good agreement with the increasing N_2 flow rate in the range of 2.5~5.0 sccm. The n and R% of $AlSi_xN_y$ increased, and the k decreased in 193 nm with the increasing of nitrogen content as shown in Fig. 2. The shift was deduced that the silicon and aluminum atoms are linked to more nitrogen atom, more silicon and aluminum nitride structures therefore formed, with the increasing of nitrogen content [3]. The n and k of silicon and aluminum nitrides which have higher n and lower k values were also indicated in Fig. 1. If the atomic percentage of nitrogen was kept in the range of 23.27%~33.26%, the transmittance T% in 365 and 488 nm is smaller than 40%., suitable for the optical inspection and alignment. When nitrogen is higher than 36.87%, the T% will rise to 60%, to high for optical inspection.

The effect of atomic percentage of silicon on n and k of $AlSi_xN_y$ was shown in Fig. 3. With the increasing of atomic percentage of silicon, the silicon nitride structure would increase in $AlSi_xN_y$, hence, the n of this film increased, and k decreased. However, when the atomic percentage of silicon increased to higher than 21%, the Si_3N_4 composition may saturate and the Si composition may rise. The n will no longer increase. The effect of atomic percentage of Al on n and k of $AlSi_xN_y$ was shown in Fig. 4. When the atomic percentage of Al increased with the increasing of Al target power, the optical properties of $AlSi_xN_y$ thin films will shift to as Al structure. In this case, the n decreased, and k increased in 193 nm. The average atomic ratio of $AlSi_xN_y$ films within the required R% and T% window is $AlSi_{0.31}N_{0.45}$, analyzed by EPMA.

Because of expensive ArF 193 nm Laser is not available, a ~254 nm broad band deep UV lamp was used instead to examine the exposure durability of these thin films. Irradiation doses up to 1 kJ/cm^2 in nitrogen environment, optical properties of $AlSi_xN_y$ thin films showed only a very slight change.

The optical properties of $AlSi_xN_y$ films are quite stable after three consecutive cleaning steps as shown in Table 1.

3.2 Etching Characterization

The using of low pressure, high density plasma etchers and chemically amplified resists could improve the resolution of patterns on mask significantly. A helicon wave etcher and a chemically amplified negative resist NEB-22 (Sumitomo) were used in this study. Several chlorine-based etchants were tested. Finally, a mixture of BCl_3, Cl_2 and O_2 was found to have better dry etching performance.

L9 orthogonal arrays of Taguchi method has been applied to optimize the etching selectivity of $AlSi_xN_y$ over substrate fused silica (SiO_2) and resist NEB-22 as outlined in Table 2. The flow ratio of BCl_3/Cl_2, flow rate of oxygen and chamber pressure are all very critical to the etching selectivity as shown in Fig. 5 and 6. The effect of RF bias is not so critical in the usual range used.

The Cl radical is the major radical to react with $AlSi_xN_y$, the Cl radical density will increase as Cl_2 flow rate increased. When flow rate was higher than 7 sccm, the chamber pressure also increased, leading the Cl radical density decreased accordingly.

Table 1. Clearing durability of $AlSi_xN_y$ embedded material with three steps in 193 nm

	80 W O_2 plasma for 5 min	SVC-150 resist stripper at 80℃ for 30 min	DI water with ultrasonic at 80℃ for 30 min
Change of T%	0.5	0.7	0.3
Change of R%	0.3	0.5	0.2
Change of thickness	1.1 nm	0.7 nm	0.5 nm

Table 2. Range of etching process parameters for Taguchi design of experiment

Level	A. Bias RF (W)	B. O_2 (sccm)	C. BCl_3/Cl_2 (sccm/sccm)	D. Pressure (mTorr)
Level 1	30	0	45/13	5
Level 2	80	4	29/29	7
Level 3	130	8	13/45	9

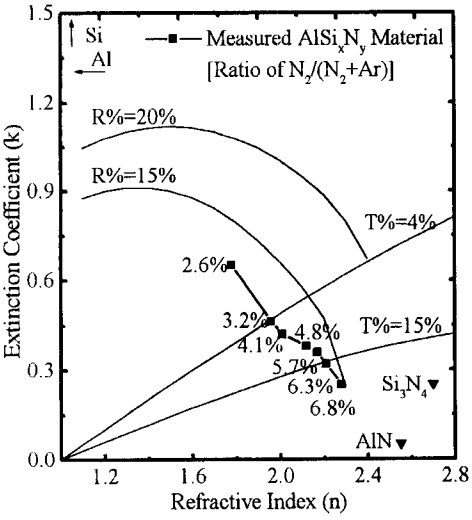

Fig. 1 n, k plane of $AlSi_xN_y$ in 193 nm under various ratios of $N_2/(Ar+N_2)$ as indicated by percentages.

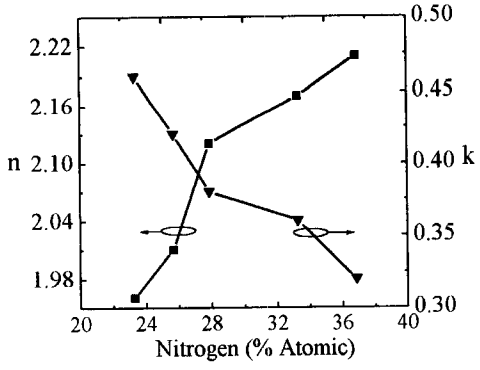

Fig. 2 The effect of atomic percentage of nitrogen on n and k of $AlSi_xN_y$ films in 193 nm under Al 130 W, Si 40 W, Ar 75 sccm and N_2 2.5~5 sccm.

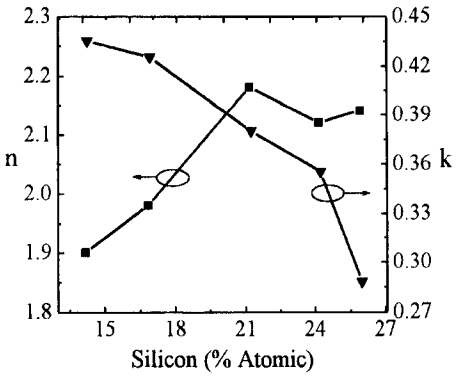

Fig. 3 The effect of atomic percentage of silicon on n and k of $AlSi_xN_y$ films in 193 nm under Al 130 W, Si 20~60 W, Ar 75 sccm and N_2 3 sccm.

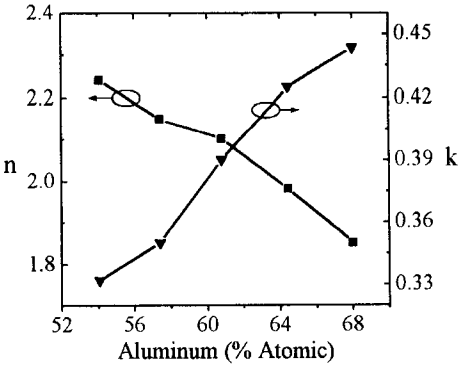

Fig. 4 The effect of atomic percentage of aluminum on n and k of $AlSi_xN_y$ films in 193 nm under Al 100~140 W, Si 40 W, Ar 75 sccm and N_2 3 sccm.

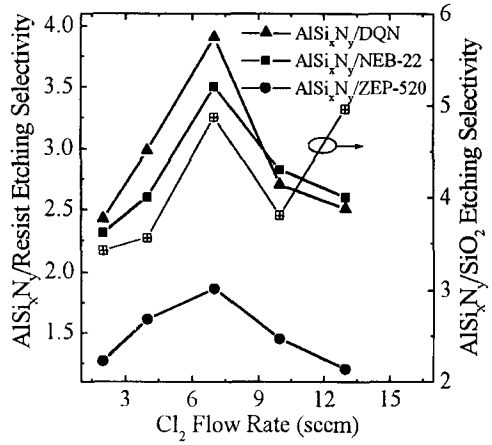

Fig. 5 The selectivity of $AlSi_xN_y$ under chamber pressure 5 mtorr, BCl_3 45 sccm, plasma source power 1400 W and substrate bias RF power 30 W.

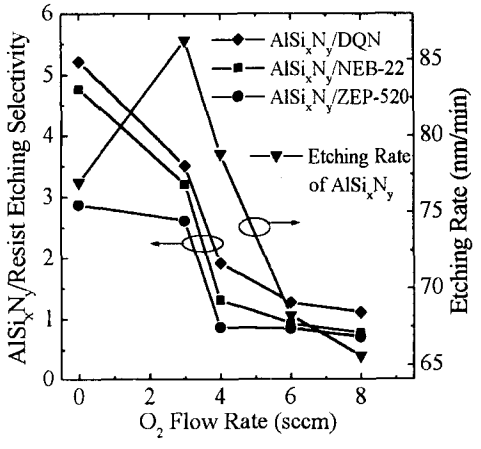

Fig. 6 Etching rate and selectivity of $AlSi_xN_y$ against O_2 flow rate under chamber pressure 3 mtorr, BCl_3 45 sccm, Cl_2 7 sccm, plasma source power 1400 W and substrate bias RF power 30 W.

Fig. 7 SEM of a 0.3 μm line/space etched pattern of $AlSi_xN_y$ as an embedded layer.

$AlSi_xN_y$ etching rate decreased due to the decreasing of Cl radical density. However, the chamber pressure had only little effect on etching rate of these resists studied. Fig. 6 showed $AlSi_xN_y$ etching rate and the selectivity of $AlSi_xN_y$ over resists against O_2 flow rates. The addition of a small amount of O_2 into the BCl_3/Cl_2 will enhance the Cl radical generation by the oxidation of BCl_x [6]. As O_2 was added into the BCl_3/Cl_2 plasma, the $AlSi_xN_y$ etching rate first increased, peaked at 3 sccm O_2, then decreased considerably. The oxidation of resists increased by O_2 addition, the etching rate of resists increased. The corresponding etching selectivity over resists decreased from 5.3 to 0.7 with the increasing of O_2 flow. NEB-22 has enough resistance to plasma etching for mask fabrication, similar to DQN/Novolak, and better than ZEP-520.

3.3 Etched Pattern

The selectivity of $AlSi_xN_y$ over NEB-22 was 4.8:1 under optimal conditions of chamber pressure 3 mtorr, BCl_3 45 sccm, Cl_2 7 sccm, plasma source power 1400 W and substrate bias RF power 30 W. The selectivity of $AlSi_xN_y$ over fused silica was 12.3:1 under chamber pressure 9 mtorr, BCl_3 13 sccm, Cl_2 45 sccm, O_2 8 sccm, plasma source power 1400 W and substrate bias RF power 30 W. Two etching steps are needed for pattern transfer. A 0.3 μm line/space etched pattern of $AlSi_xN_y$ thin film as embedded layer was illustrated in Fig. 7.

4. Conclusions

The helicon wave etcher and Taguchi design of experiment have been successfully applied to the fabrication of AttPSM using $AlSi_xN_y$ as embedded layer. $AlSi_xN_y$ thin film has the potential as a good embedded material for AttPSM in 193 nm.

References

[1] W. A. Loong et al., Microelectronic Engineering, Vol. 41/42, p. 125 (1998); Vol. 46, p. 93 (1999); Proc. SPIE, Vol. 2726, p. 524 (1996).
[2] B. W. Smith et al., J. Vac. Sci. Technol., B, Vol. 14 (6), p. 3719 (1996).
[3] F. Gaillard et al., J. Vac. Sci. Technol., A, Vol. 15 (5), p. 2777 (1997).
[4] T. Banjo et al., Jpn. J. Appl. Phys., Part 1, Vol. 36, No. 7B, p. 4824 (1997).